

ENC-2022-0309

THE EFFECT OF RHEOLOGICAL PROPERTIES OF NON-NEWTONIAN FLUIDS ON THE AMPLIFICATION RATE OF ROLL WAVES IN FREE-SURFACE FLOWS

Valdirene da Rosa Rocho
Guilherme Henrique Fiorot
Sergio Viçosa Möller

valdirenerocho@gmail.com
guilherme.fiorot@ufrgs.br
svmoller@ufrgs.br

Mechanical Engineering Graduate Program - PROMEC, Mechanical Engineering Department, Federal University of Rio Grande do Sul

Abstract. *Due to their complex nature, non-Newtonian fluids can be present in the most diverse types of flows. The behavior of these fluids is subject to various dynamic conditions that must be controlled to ensure no distortions in the flow. Furthermore, these flows can develop instabilities during their temporal-spatial evolution; thus, it is necessary to understand how this evolution occurs. This paper presents a linear stability analysis for free-surface flows considering a power-law fluid. The analysis is performed to verify the flow stability and obtain the wave growth rate from flow parameters. Firstly, through the perturbation method, a linear stability analysis was performed to obtain the marginal stability curve and the wave growth rate. From this analysis, it was possible to establish the domain suitable for the generation of roll waves as a function of the Froude number and fluid index flow. This study aims to evaluate the rheological effect of non-Newtonian properties on the amplification rate and to obtain indications about the development of roll waves as a function of such parameters. From the obtained functions, it was possible to make a comparative analysis, identifying and separating the effect of the flow index on the evolution of the flow instabilities.*

Keywords: *free-surface flow, stability analysis, power-law fluid, roll waves.*

1. INTRODUCTION

In fluid flows in inclined and open channels there is usually generation and propagation of a train of waves, either naturally arising or formed by the introduction of a disturbance applied to the flowing fluid. In these scenarios, the flows may present sufficient conditions over time to develop the presence of hydrodynamic instabilities.

The fundamentals of the theory of hydrodynamic instability have been examined since the time of Osborne Reynolds (Charru, 2011). Currently, the study of hydrodynamic instabilities has been of utmost importance, given the relevance of understanding how their evolution occurs in time and space making it possible to obtain control of the flow properties (Needham and Merkin, 1984; Pascal, 2006).

During the evolution process of surface flows, if sufficient conditions exist and the introduction of a disturbance is applied properly, a wave train will propagate faster than the flow. In specific cases, this instability in the form of a wave train is called a roll wave. These waves arise from the equilibrium caused by gravitational and viscous forces acting on the flow, forming a well-defined wave train on the free surface of the flow (Zanuttigh and Lamberti, 2007, 2010; Maciel *et al.*, 2013).

Theoretically, the study of roll waves has been conducted for many decades, since Jeffreys (1925) and Dressler (1949) and was extended by Ishihara *et al.* (1954) who considered the case of a flow with the development of roll waves in the laminar regime. His study was grounded in a theoretical and numerical approaches. The simulations were conducted considering the flowing fluid as water under thin-film conditions. From the results of the simulations, the authors found that the flow is susceptible to the formation of roll waves if the Froude number is greater than $1/\sqrt{3}$, a necessary but not sufficient condition for the formation of these waves. In addition, the authors realized that there is a minimum channel length required for these instabilities to develop; that demonstrates the great interest in engineering in understanding the

formation and propagation of these waves.

Contributing to these results, Tamada and Tougou (1979) also performed a stability analysis, identifying the characteristic properties of the waves, and validating the developed theory through numerical experiments. Continuing the work on roll waves in laminar flows, Julien and Hartley (1986) investigated the roll waves problem on the strand experimental using a smooth inclined channel. The authors explored different scenarios for hydraulic configurations in distinct types of flow, highlighting the subcritical and supercritical cases. In addition, they were able to quantify important properties such as the growth rate of the disturbances together with the properties of the generated waves and compare them with the results of the theory already developed.

More recently, the study regarding the theory of roll wave instabilities has been developed by several authors: Tamada and Tougou (1979), Ng and Mei (1994), Liu (1994), Pascal (2006), Maciel *et al.* (2013), Di Cristo *et al.* (2017), among others. These authors have studied the theory by employing more complex rheological models, for example, power law, Bingham, and Herschel-Bulkley. Due to the inherent difficulty of free surface models, these studies were conducted using a linear stability analysis, seeking to establish, as in previous works, the limits of stability of the system and its amplification rates. This analysis allowed obtaining parameters for more specific control of the minimum Froude number and thus obtaining indicators for the generation of roll waves. Although the stability limits can be obtained mathematically, the wave properties (length, profile, etc.) are obtained through the numerical solution of the mathematical models and the roll waves equation (Maciel *et al.*, 2013).

More specifically, the existing theoretical models are based on simplifications of the conservation equations of the problem. The governing equations are vertically integrated and then subjected to the application of boundary conditions. The system thus obtained is a Saint-Venant type system, widely used in hydraulic problems. The model predicts from the space-time linear stability analysis a minimum Froude number for the onset of instability (Liu, 1994; Ng and Mei, 1994; Balmforth and Liu, 2004; Di Cristo and Vacca, 2005; Maciel *et al.*, 2013).

Within this context, Ng and Mei (1994) presented a mathematical modeling with a rheological power-law type proposal, starting from the shallow water formulation for laminar flow they established the propitious domain ($F > F_{\min}$) for roll wave generation as a function of Froude number.

Extending the work of Ng and Mei (1994), Pascal (2006) studied the same instabilities but considered a channel with a porous bottom. Again, stability analyses were conducted to numerically observe the formation of roll waves, and determine the main characteristics of the phenomenon, such as wave height, length, and propagation velocity. Pascal (2006) complemented the stability analysis by also conducting a nonlinear analysis, from which he observed the nonlinear evolution of the infinitesimal perturbation imposed on uniform flow.

Later, Longo (2011), extending the theory of Dressler (1949), studied free surface instabilities in granular flow. In the analysis, the author assumed that the grains behaved as a power-law type fluid. The work developed by Longo (2011) refers to an analytical study and presents existing conditions for roll waves to exist. One of the important considerations, presented by the author, is that due to the type of functions obtained, no periodic solution is predicted for the wave profile.

Di Cristo *et al.* (2017) investigated the spatial evolution of natural roll waves in a power-law fluid using numerical experiments. The authors' goal in performing this work was to verify the influence of the boundary condition at the flow inlet. Among the results obtained, the authors pointed out that the linearized model describes the spatial growth of the roll waves in the first phase of their formation. And the main conclusion was that the spatial evolution of these waves is strongly affected by the initial profile, in which they suggested that there is a passive control utilizing inlet operations. This control may be an effective and promising strategy in the natural development of roll waves.

In this context, the present work focuses on the theoretical approach to the rolling wave problem for a fluid of non-Newtonian rheology of the power-law type. First, we re-conduct the classical linear stability analysis to obtain a curve for the temporal and spatial growth rate of the waves. From the case study, the goal is to evaluate the effect that the flow rate of the fluid has on the spatial/temporal growth of the roll waves.

2. METHODOLOGY

In the present work, an analytical mathematical model based on the Cauchy equations with a power-law rheological model was employed to model free surface fluid flow (Ng and Mei, 1994; Liu, 1994; Pascal, 2006; Maciel *et al.*, 2013).

2.1 Rheological model

Fluids are said to be non-Newtonian when the relationship between stress and strain is no longer represented by a linear relationship. There are many examples of such fluids, for example, polymers. This kind of material can have a Newtonian representation only for low or high strain rates. Their global behavior cannot be represented by a simple linear relationship, i.e., they do not obey Newton's law of viscosity; therefore, other concepts must be used for their characterization. There are several factors that influence the viscosity of fluids; among them are the temperature, pressure, shear rate, and shear time (Irgens, 2014). Considering a power-law rheology model, which is the model used to represent fluids that present behavior where shear rate is dependent on the shear stress, the constitutive relationship (in simple shear

conditions) can be given by:

$$\tau_{xz} = \mu_n \left(\frac{\partial u}{\partial z} \right)^n \quad \text{with } 0 < n \leq 1, \quad (1)$$

where, τ_{xz} the shear stress acting in the longitudinal direction x due to gradient at z , u the velocity component at x , z the coordinate in the vertical direction, $\partial u / \partial z$ is the fluid strain rate, μ_n is the fluid consistency index and n is the flow index.

2.2 Description of the mathematical model – governing equations

The phenomenon was studied for laminar flow in which the flowing fluid has non-Newtonian rheology, more precisely, the power-law type. Classical conservation equations were used for this analysis, i.e., the Cauchy equations. Therefore, to simplify, it was necessary to define boundary conditions appropriate to the problem and some simplifying hypotheses.

The general scheme of the problem studied in the presence of roll waves type instabilities is represented by Fig. 1.

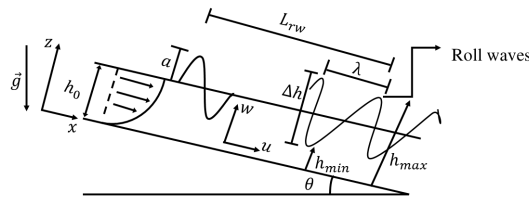


Figure 1: General scheme of free-surface flow.

Figure 1 illustrates the geometry of the studied problem for a 2D velocity field (u, w) , where u is the longitudinal velocity in the x coordinate direction of the channel, and w is the vertical velocity in the z coordinate direction of the channel, h_0 is the depth of the uniform flow, a is the amplitude of the disturbance, Δh is the amplitude of the wave, h_{\min} is the depth referring to the wave trough (minimum flow height), h_{\max} the depth referring to the wave crest (maximum flow height), L_{rw} is the minimum longitudinal distance, λ is the wavelength, $g = 9.81 \text{ m/s}^2$ is the acceleration of gravity and θ is the channel slope.

The problem was simplified under the following assumptions: the flow occurs by the action of gravity applied in the plane (x, z) ; homogeneous, incompressible fluid with constant specific mass ρ ; shallow water conditions, i.e., depth of flow h is much smaller than the characteristic longitudinal length L ; infinitely wide channel, flow depth h much smaller than channel width W ; fixed channel bottom; there is no exchange of momentum quantity between fluids (liquid and gas); laminar regime (Maciel *et al.*, 2013).

After the hypotheses are established, the boundary conditions are defined. Among them define the kinematic conditions at the free surface (Eq. 2) and the no-slip and impermeability boundary conditions at the bottom of the channel (Eq. 3), i.e.:

$$w(z) = \frac{\partial h}{\partial t} + u(z) \frac{\partial h}{\partial x}, \quad \text{to } z = h(x, t), \quad (2)$$

$$u(z) = w(z) = 0, \quad \text{to } z = 0. \quad (3)$$

The free surface stress is given by:

$$p(z) = 0, \quad \tau_{xz}(z) = 0, \quad \frac{\partial u}{\partial z} = 0 \quad \text{to } z = h(x, t); \quad \text{and } \tau_{xz}(z) = \tau_p, \quad \text{to } z = 0, \quad (4)$$

where τ_{xz} characterizes the shear stresses acting in the longitudinal x direction due to the gradient in the z direction, and t is time.

Following the same formalities described in the literature, the simplification of the problem was made (Ng and Mei, 1994; Balmforth and Liu, 2004; Di Cristo and Vacca, 2005; Maciel *et al.*, 2013). Next, the equations for conservation of mass and momentum along the depth (h) of the flow were solved, and then the boundary conditions (Eqs. 2 and 3) were applied by integrating the following equations (Eqs. 5, 6 and 7):

$$\frac{\partial u}{\partial x} + \frac{\partial w}{\partial z} = 0, \quad (5)$$

$$\rho \left(\frac{\partial u}{\partial t} + u \frac{\partial u}{\partial x} + w \frac{\partial u}{\partial z} \right) = - \frac{\partial p}{\partial x} + \rho g \sin \theta + \frac{\partial \tau_{xz}}{\partial z}, \quad (6)$$

$$\frac{\partial p}{\partial z} = -\rho g \cos \theta, \quad (7)$$

where p is the pressure.

Solving the system of equations (Eqs. 5, 6 and 7) vertically and applying the boundary conditions results the following system of equations:

$$\frac{\partial \bar{u}h}{\partial x} + \frac{\partial h}{\partial t} = 0 \quad (8)$$

$$\frac{\partial \bar{u}h}{\partial t} + \frac{\partial}{\partial x} (\alpha \bar{u}^2 h) + \frac{\partial}{\partial x} \left(g \cos \theta \frac{h^2}{2} \right) = gh \sin \theta - \frac{1}{\rho} \tau_p, \quad (9)$$

where h is the flow depth, \bar{u} is the vertical mean velocity, α is the velocity distribution coefficient and τ_p is the channel bottom shear stress. Surface stress is neglected because the remaining shear stress is the shear stress at the bottom of the channel where $\tau_p = \tau_{xz}$ ($z = 0$).

In order to study the physical/mathematical problem, the variables that make up the system were written in dimensionless form. The following dimensionless scales were adopted (Ng and Mei, 1994; Maciel *et al.*, 2013): length scale – $x = Lx^*$, $h = h_0 h^*$ e $y = h_0 y^*$; velocity scale – $\bar{u} = \bar{u}_0 \bar{u}^*$; time scale – $t = L/\bar{u}_0 t^*$.

Furthermore, the Froude number (F) is given by: $F = \frac{\bar{u}_0}{\sqrt{gh_0 \cos \theta}}$, where \bar{u}_0 is the average velocity in the longitudinal x direction. As for the subindices, ()₀ indicates the uniform flow conditions, and ()^{*} the asterisk represents the dimensionless variables. Since this is a power-law rheological model flow the shear stress is represented by Eq. (1).

The dimensionless variables were included in the system (Eqs. 8 and 9), leading to a new system of differential equations, is given by:

$$\frac{\partial h}{\partial t} + \frac{\partial u h}{\partial x} = 0 \quad (10)$$

$$h \left(\frac{\partial u}{\partial t} + \alpha u \frac{\partial u}{\partial x} \right) + u (1 - \alpha) \frac{\partial h}{\partial t} + \frac{h}{F^2} \frac{\partial h}{\partial x} = h - \left(\frac{u}{h} \right)^n, \quad (11)$$

with $\alpha = 2 \left(\frac{2n+1}{3n+2} \right)$. It is worth mentioning that in this work the asterisks and bars of the equations of conservation of mass and momentum were neglected after obtaining the system in its dimensionless form. Based on the mathematical model obtained, it was possible to search for favorable conditions for the formation of instabilities.

2.3 Linear stability analysis

In carry out a linear stability analysis using the system of equations (Eqs. 10 and 11), guiding information on the flow stability conditions was sought, that is, what are the stability criteria for the generation roll waves instabilities. To determine these criteria, it was necessary to analyze the temporal and spatial growth rates.

To perform linear stability analysis, an infinitesimal perturbation of small amplitude is added to the uniform flow in the mass and momentum conservation equations ((h, u) = (1, 1)), where: $h(x, t) = 1 + \hat{H}(x, t)$ and $u(x, t) = 1 + \hat{U}(x, t)$.

Taking into account that $|\hat{H}(x, t)| \ll 1$ and $|\hat{U}(x, t)| \ll 1$ the Eqs. (10) and (11) can be rewritten as:

$$\frac{\partial \hat{H}}{\partial t} + \frac{\partial \hat{U}}{\partial x} + \frac{\partial \hat{H}}{\partial x} = 0, \quad (12)$$

$$\frac{\partial \hat{U}}{\partial t} + \alpha \frac{\partial \hat{U}}{\partial x} + \frac{1}{F^2} \frac{\partial \hat{H}}{\partial x} + (1 - \alpha) \frac{\partial \hat{H}}{\partial t} = 1 - \left(\frac{1 + \hat{U}}{1 + \hat{H}} \right)^n. \quad (13)$$

From Eqs. (12) and (13) some algebraic manipulations based on the linearization technique were done, and thus a single differential equation for $\hat{H}(x, t)$ is obtained:

$$\frac{\partial^2 \hat{H}}{\partial t^2} + \left(\alpha - \frac{1}{F^2} \right) \frac{\partial^2 \hat{H}}{\partial x^2} + 2\alpha \frac{\partial^2 \hat{H}}{\partial t \partial x} + n \frac{\partial \hat{H}}{\partial t} + (2n+1) \frac{\partial \hat{H}}{\partial x} = 0 \quad (14)$$

Equation (14) is a partial differential equation that describes the propagation of waves. The interest in developing this work was to obtain the conditions for the generation of roll waves, and the particularity of these waves is the periodicity. Thus, it is considered that the solution of Eq. (14) is of the type (Briggs, 1964; Ng and Mei, 1994; Maciel *et al.*, 2013):

$$\hat{H}(x, t) = |H(x, t)| e^{i(\omega t - kx)} \quad (15)$$

where $\hat{H}(x, t)$ is the perturbation magnitude, k the wavenumber and ω is the wave frequency, these are usually complex numbers.

According to the linear stability theory which consists in conjecturing the existence of perturbations. The high-order terms were neglected and the solutions are defined as elementary waves where $k = k_r + ik_i$, the complex wavenumber, and $\omega = \omega_r + i\omega_i$, complex frequency.

To perform the stability analysis, Eq. (15) is inserted into (14) and the quadratic equation is obtained, which is called the dispersion equation (Eq. 16):

$$\omega^2 + \left(\alpha - \frac{1}{F^2} \right) k^2 - 2\alpha k\omega - in\omega + i(2n + 1)k = 0. \quad (16)$$

From the dispersion equation it was possible to observe the temporal ($k = k_r$ and $k_i = 0$) and spatial ($\omega = \omega_r$ and $\omega_i = 0$) evolution of the instabilities (Briggs, 1964; Huerre and Monkewitz, 1990; Maciel *et al.*, 2013).

The development of this work aims to reevaluate the stability analyses already conducted in the literature by Liu (1994), Ng and Mei (1994), Di Cristo and Vacca (2005), Maciel *et al.* (2013), among others, and from these observe how the evolution of the growth rates of instabilities occurs. It is worth mentioning that the whole mathematical procedure will be considered as a result of this work.

3. RESULTS

3.1 Temporal stability analysis

The temporal stability analysis was performed from the dispersion equation (Eq. 16). For this investigation, it was considered that $k = k_r$ which was solved for the variable ω . This way we obtain the solution of Eq. (17), known as the temporal branch. By the quadratic characteristic of Eq. (16) we obtain a pair of complex functions that depend mainly on the number of waves.

$$\omega(k) = \alpha k + \frac{ni}{2} \pm \sqrt{k^2 \left(\alpha^2 - \alpha + \frac{1}{F^2} \right) + ik [n(\alpha - 2) - 1] - \frac{n^2}{4}} \quad (17)$$

From Eq. (17), two solutions are obtained, in which they have been separated into an imaginary part and a real part, according to Eqs. (18) and (19):

$$\omega_i(k) = \frac{n}{2} \pm \frac{1}{4} \sqrt{-8k^2 \left(\alpha^2 - \alpha + \frac{1}{F^2} \right) + 2n^2 + 8 \sqrt{\left[k^2 \left(\alpha^2 - \alpha + \frac{1}{F^2} \right) - \frac{n^2}{4} \right]^2 + (k\alpha n - k(2n + 1))^2}}, \quad (18)$$

$$Re\{\omega(k)\} = \alpha k \pm \frac{1}{4} \sqrt{8k^2 \left(\alpha^2 - \alpha + \frac{1}{F^2} \right) - 2n^2 + 8 \sqrt{\left[k^2 \left(\alpha^2 - \alpha + \frac{1}{F^2} \right) - \frac{n^2}{4} \right]^2 + k^2(\alpha n - 2n - 1)}}. \quad (19)$$

As for the existence of instability, it is represented by the imaginary part of the pair of branches $\omega(k)$, these make up the temporal growth rate of instabilities (Briggs, 1964; Huerre and Monkewitz, 1990; Ng and Mei, 1994; Maciel *et al.*, 2013). To determine the condition for generating instabilities related to the Froude number (F), the following inequality is considered:

$$\omega_i(k) < 0. \quad (20)$$

From the solution of Eq. (20) we obtain the criterion necessary for the formation of roll waves, which depends on F (see Eq. 21), i.e.,

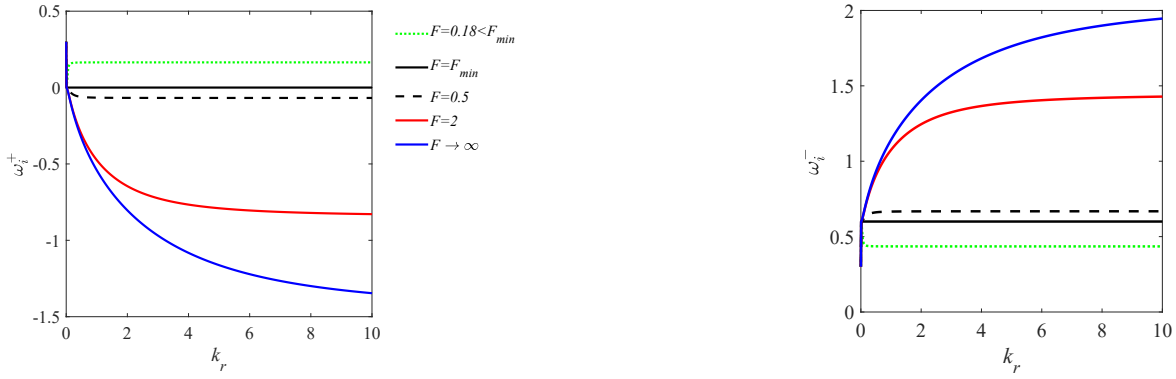
$$F = \frac{n}{\sqrt{2n + 1}}. \quad (21)$$

Under these conditions, the domain favorable to the propagation of instabilities can be obtained when:

$$F > F_{\min} = \frac{n}{\sqrt{2n + 1}}, \quad (22)$$

that is, this control parameter indicates that there is a minimum Froude number, F_{\min} , above which instabilities will be amplified in this system. A similar analysis was proposed by Ng and Mei (1994), Di Cristo and Vacca (2005), Pascal (2006) and Maciel *et al.* (2013).

The parameter F_{\min} depends on the flow index n and according to Ng and Mei (1994) the region in which one obtains a domain favorable to instability generation for shear-thinning-type fluid occurs when $0 < n \leq 1$. In Fig. 2 the growth



(a) Positive branches.

(b) Negative branches.

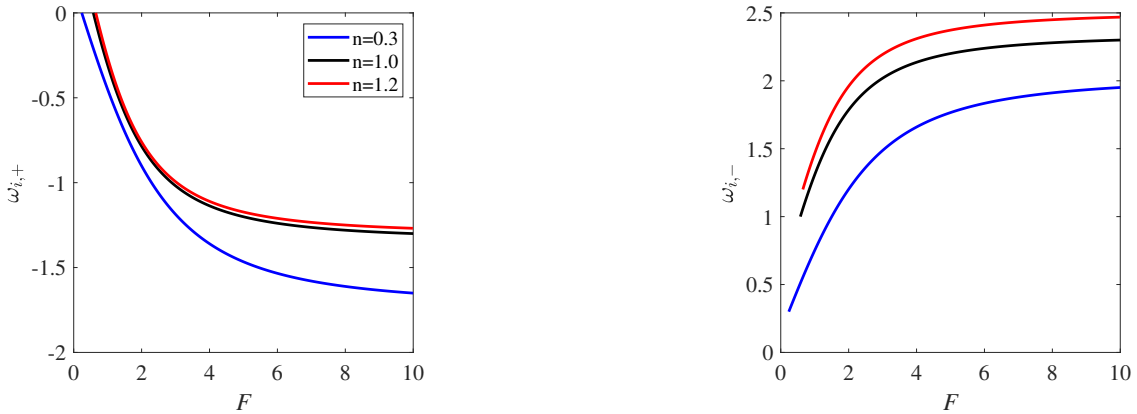
Figure 2: The temporal growth rate of disturbances for a power-law fluid for fixed power index at different F .

rate of the perturbations for positive and negative branches is illustrated. To obtain these we fixed the parameter $n = 0.6$ and varied the Froude number, in this case, $F_{\min} = 0.40$.

Based on Fig. 2 it was noted that for different Froude numbers two temporal branches coexist, this fact occurs due to the quadratic characteristic of the dispersion equation (Eq. 16). It was also observed that there is an amplification of the disturbance only when $F > F_{\min}$. This fact occurs for the positive branch (Fig. 2a). Furthermore, through Fig. 2 it was possible to notice that for $k \rightarrow +\infty$ the amplification rate has asymptotic behavior and that the growth rate of the instabilities decreases with the increasing wavenumber. Taking this consideration into account, a mathematical expression was sought to determine the numerical value for this rate which was obtained by means of limit values, i.e:

$$\lim_{k \rightarrow +\infty} \omega_{i,+} = \frac{n}{2} + \frac{n(\alpha - 2) - 1}{2\sqrt{\alpha^2 - \alpha + \frac{1}{F^2}}}. \quad (23)$$

Still, referring to the amplification rate, a second analysis was performed to evaluate the influence of the parameter n on the temporal growth rate when $k \rightarrow +\infty$ and $k \rightarrow 0$ as a function of the Froude number. For such an analysis the effect and contribution that this term presents when $F > F_{\min}$ was weighted. Figure 3 illustrates the temporal growth rate of the perturbations for short waves ($k \rightarrow +\infty$).



(a) Positive branches.

(b) Negative branches.

Figure 3: The temporal growth rate of perturbations for short waves ($k \rightarrow +\infty$) in a power-law fluid with different flow index (n) as a function of the Froude number.

According to Fig. 3, the amplification of the perturbation only happens for the positive temporal branch. It was observed that the parameter n influences the growth rate increase as n grows. Still, it is worth noting that for $n = 1$ we are dealing with the fluid Newtonian rheology. When $n = 0.3 < 1$, the viscosity of the fluid comes into play, which will be inversely proportional to the shear rate, and it is classified as a pseudoplastic fluid. And in the case where $n = 1.2 > 1$ the viscosity is directly proportional to the shear rate, so the fluid is dilatant (Irgens, 2014). Even though there are these rheological differences in the fluid the behavior of the stability curves is similar.

Figure 4 shows numerically the growth rate of the disturbances for long waves ($k \rightarrow 0$) as a function of the Froude number, for various values of n .

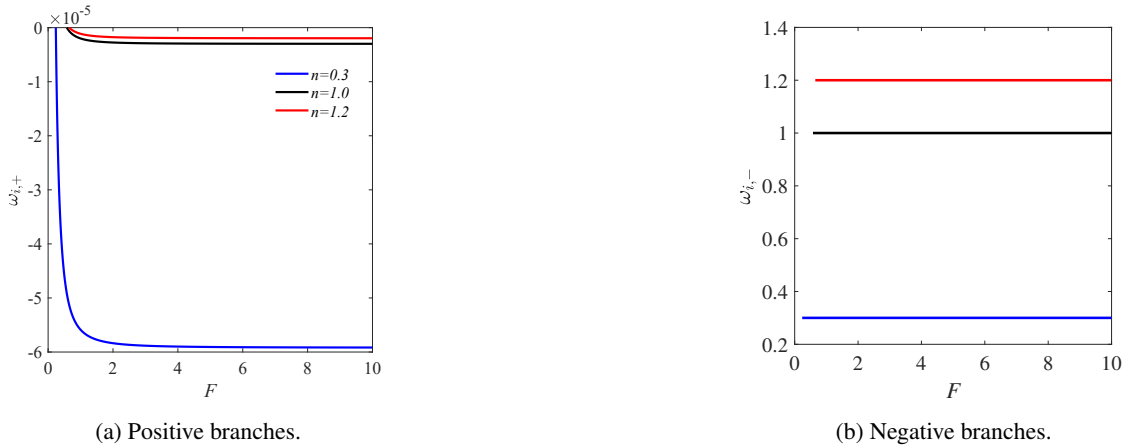


Figure 4: The temporal growth rate of perturbations for long waves in a power-law fluid with different flow index (n) as a function of the Froude number.

By fixing the value of the parameter n , one can check the influence of this index on the temporal growth rate of the disturbances when $k \rightarrow 0$. It can be seen from Fig. 4 that for the negative branch (Fig. 4b) the temporal growth rate corresponds to the value of the flow index n . To have wave amplification $\omega_i < 0$, otherwise, the waves do not amplify. Looking at Fig. 4(a) it can be seen that the amplification rate is very low when $k \rightarrow 0$, i.e., $\omega_{i,+} \rightarrow 0$. Furthermore, if we combine Figs. 3(a) and 4(a) the temporal growth rate for $0 < k < +\infty$ assumes values approximately between $[-2, 0]$.

3.2 Spatial stability analysis

The spatial stability analysis was performed in order to evaluate the evolution of roll waves in space. For this, it was necessary to determine the spatial branches $k(\omega)$ (Eq. 24) that refer to cases in which the complex wavenumber k is determined as a function of a complex frequency ω .

$$k(\omega) = \frac{2\alpha\omega - i(2n+1) \pm \sqrt{4\omega^2 \left(\alpha^2 - \alpha + \frac{1}{F^2}\right) + 4\omega i \left[\alpha n - \alpha(2n+1) - \frac{n}{F^2}\right] - (2n+1)^2}}{2 \left(\alpha - \frac{1}{F^2}\right)}. \quad (24)$$

Analogous to the temporal stability analysis, the spatial growth rate was determined. For $k_i(\omega) > 0$, the perturbations are amplified in space. From Eq. (24) the solution is obtained separately, i.e., the imaginary part and real part in accordance with Eqs. (25) and (26).

$$k_i(\omega) = \frac{-(2n+1) \pm \sqrt{\frac{\sqrt{[4\omega^2(\alpha^2 - \alpha + \frac{1}{F^2}) - (2n+1)^2]^2 + 16\omega^2[\alpha(n+1) + \frac{n}{F^2}]^2 - 4\omega^2(\alpha^2 - \alpha + \frac{1}{F^2}) + (2n+1)^2}}{2}}}{2 \left(\alpha - \frac{1}{F^2}\right)} \quad (25)$$

and

$$Re\{k(\omega)\} = \frac{2\alpha\omega \pm \sqrt{\frac{\sqrt{[4\omega^2(\alpha^2 - \alpha + \frac{1}{F^2}) - (2n+1)^2]^2 + 16\omega^2[\alpha(n+1) + \frac{n}{F^2}]^2 + 4\omega^2(\alpha^2 - \alpha + \frac{1}{F^2}) - (2n+1)^2}}{2}}}{2 \left(\alpha - \frac{1}{F^2}\right)}. \quad (26)$$

The existence of the instabilities is expressed by the imaginary part of the branches (k_i). From Eqs. (25) and (26) it was observed that they present a singularity point as soon as $F^2 = 1/\alpha$. In order to determine the instability criterion, it was analyzed when $k_i(\omega) = 0$, and thus it is obtained that: $F^2 = \frac{n^2}{2n+1}$.

We reinforce that F_{\min} is the same as that obtained in the temporal stability analysis (Eq. 22). And the singularity point can be rewritten as:

$$F_s = \frac{1}{\sqrt{\alpha}}. \quad (27)$$

Based on the two established criteria, that is, minimum Froude number criterion and Froude number singularity point, it was sought to identify through these which values that F_{\min} , F_s , and α assume in the unsteady and stable regions of flow as a function of the rheological parameter n and thus perform an analysis based on the effect that this factor can cause. Such an analysis was performed by means of Fig. 5.

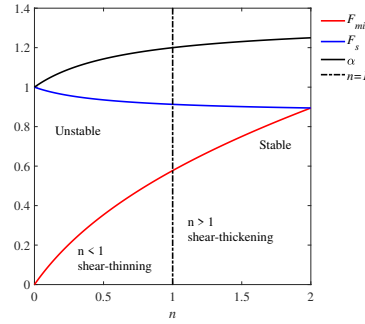


Figure 5: Geometric representation of the region favorable for propagation of roll waves as a function of the parameter n .

From Fig. 5 it is possible to identify the limits of the domain favorable to the generation of instabilities for each type of fluid, for example, when $n = 1$ the fluid is of Newtonian rheology, and we have that $F_{\min} = 1/\sqrt{3}$, $\alpha = 1.2$ and $F_s = 1/\sqrt{1.2}$. Thus, there will only be amplification of the perturbations when $F_{\min} > 1/\sqrt{3}$ (Ishihara *et al.*, 1954; Julien and Hartley, 1986). In the case where the fluid is pseudoplastic, $0 < n < 1$, it is obtained that the control parameters vary according to the following inequalities: $0 < F_{\min} < 1/\sqrt{3}$, $1 < F_s < 1/\sqrt{1.2}$ and $1 < \alpha < 1.2$; and for the dilatant fluid, $1 < n < 2$, hence, $1/\sqrt{3} < F_{\min} < 2/\sqrt{5}$, $1.2 < \alpha < 5/4$ and $1/\sqrt{1.2} < F_s < 2/\sqrt{5}$.

Given the two main criteria established (F_{\min} and F_s) we sought to evaluate the spatial growth rate ($k_i(\omega)$) as a function of frequency (ω_r) for different Froude numbers, with parameter $n = 0.6$ (shear-thinning fluid), $F_{\min} = 0.405$ and $F_s = 0.929$. Figure 6 shows the spatial growth rate of the perturbations.

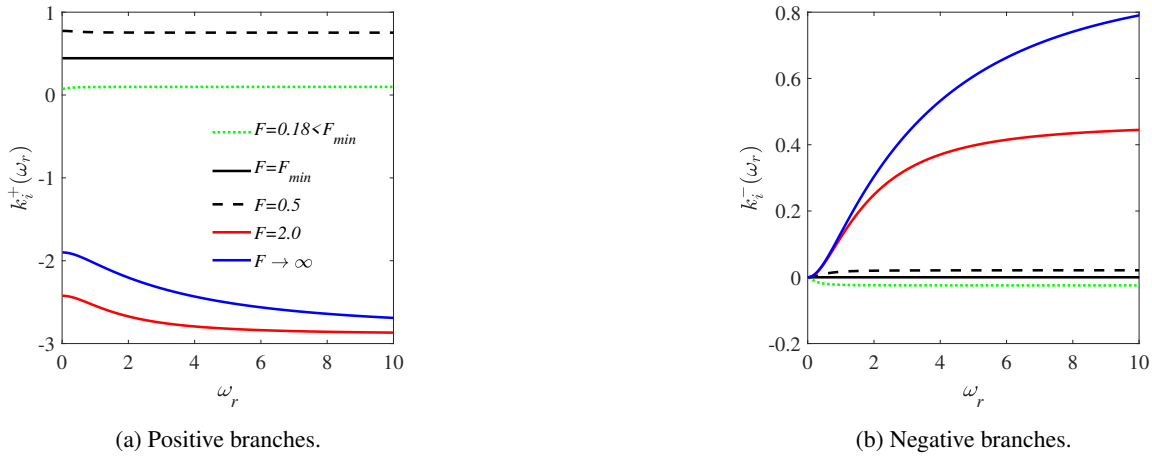


Figure 6: The spatial growth rate of disturbances for a power-law fluid for fixed power index ($n = 0.6$) at different F .

Regarding the criteria for generation and propagation of instabilities in Fig. 6, there are two situations: positive branch (Fig. 6a) – one can observe that for the domain ω_r the function $k_i(\omega_r)$ has both positive ($k_i(\omega_r) > 0$) and negative ($k_i(\omega_r) < 0$) image. Also, in relation to Fig. 6(a), it is observed that for $F \leq F_{\min}$, k_i^+ is positive and points out that there would be amplification of perturbations, however, according to the literature, the amplification of perturbations through the temporal stability analysis indicates that there will only be roll waves type instability for $F > F_{\min}$. The analysis performed from 6(a) leads to the conclusion that the classical theory of linear stability analysis points to a limitation of the mathematical model and has no physical sense when it is obtained that $F \leq F_{\min}$, k_i^+ is positive. In this case there is only amplification of the perturbations when $F_{\min} < F < F_s$. Conversely, for all cases with $F > F_s$ one gets $k_i(\omega_r) < 0$, i.e. there is no amplification of the imposed perturbation. With respect to the negative branch (Fig. 6b) there is amplification of the waves when $F > F_{\min}$.

By observing the asymptotic behavior of the spatial growth rate, $k_i(\omega_r)$, we sought to determine through the limits a function k_i when $\omega \rightarrow +\infty$ and it is given by:

$$\lim_{\omega \rightarrow +\infty} k_i = -\frac{2n+1}{2\left(\alpha - \frac{1}{F^2}\right)} \mp \frac{\alpha(n+1) + \frac{n}{F^2}}{2\left(\alpha - \frac{1}{F^2}\right) \sqrt{\alpha^2 - \alpha + \frac{1}{F^2}}}. \quad (28)$$

A second analysis was performed regarding the amplification rate $k_i(\omega_r)$ as a function of Froude number. The analysis was performed for perturbation frequency $\omega \rightarrow 0$ and $\omega \rightarrow +\infty$ for three flow rates: $n = 0.3$ ($F_s = 0.952$), $n = 1.0$ ($F_s = 0.913$) and $n = 1.2$ ($F_s = 0.908$) with $\omega \rightarrow 0$, see Fig. 7.

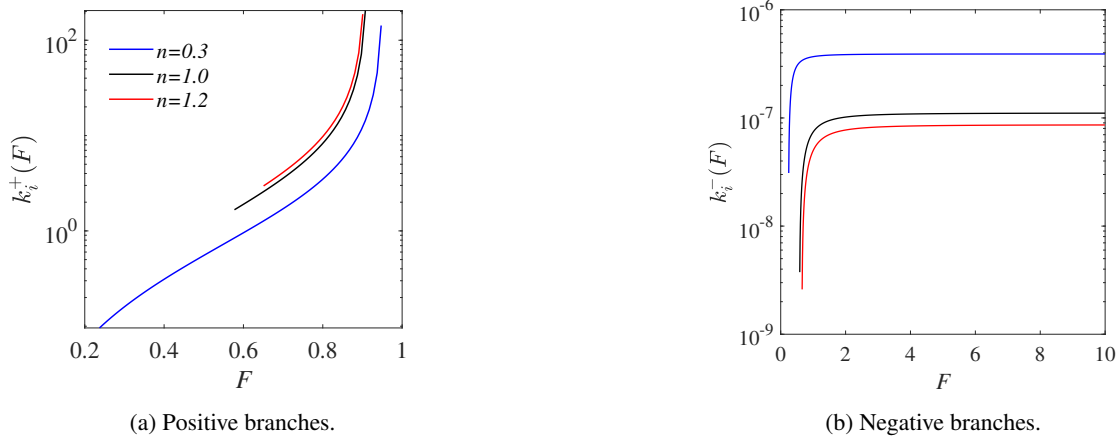


Figure 7: The spatial growth rate of disturbances for a power-law fluid with $\omega \rightarrow 0$.

Note from Fig. 7(a) that the spatial growth rate is positive only when $F_{\min} < F < F_s$. This fact is noticeable when plotting k_i on a logarithmic scale where it does not admit $k_i < 0$. In this case, one can see that the amplification of the perturbations is divided by the singularity point (F_s), because one gets propagation of the perturbations only when $F_{\min} < F < F_s$. When $F > F_s$, $k_{i,+} < 0$, and in this case the waves attenuate. From Fig. 7(b) it can be seen that the negative branch exhibits approximately zero growth rate ($k_i \rightarrow 0$) for the domain $F_{\min} < F < 10$, i.e., there is no wave propagation. With respect to the parameter n , the growth rate increases with n (Fig. 7a).

Next, we sought to evaluate the spatial growth rate of the perturbation when $\omega \rightarrow +\infty$ as a function of the Froude number for different values of n , see Fig. 8.

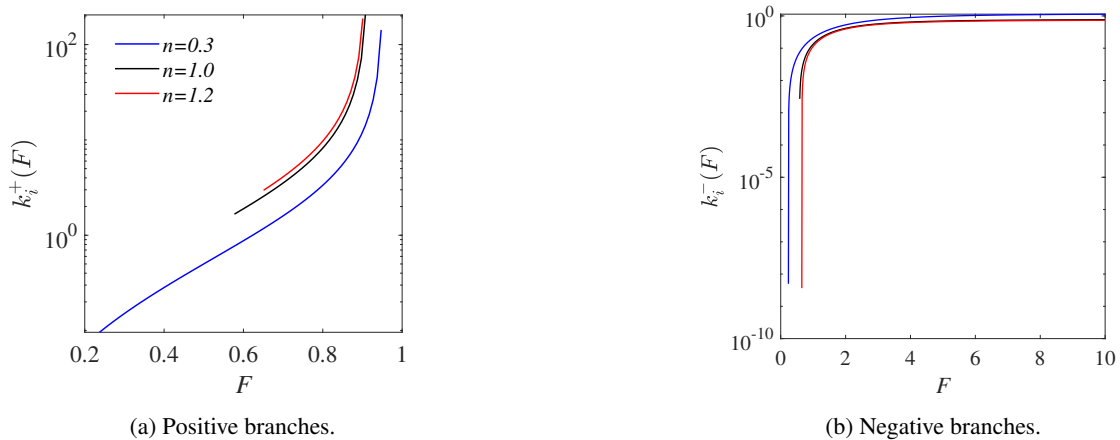


Figure 8: The spatial growth rate of disturbances for a power-law fluid with $\omega \rightarrow +\infty$.

Figure 8 shows the stability curves when $\omega \rightarrow +\infty$. Note that the amplification of the perturbations occurs for the positive branch only when $F_{\min} < F < F_s$, same observation reported earlier (Fig. 8a). Furthermore, in the case where the branch is negative, there is amplification of disturbances when $F > F_{\min}$ where $k_i \rightarrow 1 > 0$. As for the parameter n , it can be seen in Fig. 8(a) that, as n grows, $k_{i,+}$ also grows. In the case in Fig. 8(b), the opposite occurs.

4. CONCLUSION

In this work, a space-temporal linear stability analysis was applied to the system of equations obtained from the equations of conservation of mass and momentum for a surface flow of a power-law fluid, which provided control parameters for the propagation of roll waves hydrodynamic instabilities. The results of the stability analysis were explored as a function of the parameter that characterizes fluids with the indicated rheological behavior: the flow index n .

First, the results of the temporal analysis showed that the temporal growth rate ($\omega_i(k_r)$) strongly depends on the wavenumber and the control parameter F . The results found through this analysis corroborate with those already found in the literature, which show the existence of F_{\min} necessary, but not sufficient, for the propagation of instabilities to be amplified by the flow. The amplification limits were identified as a function of threshold values for the wavenumber ($k \rightarrow 0$ and $k \rightarrow +\infty$). It was possible to observe that the flow index presents a considerable influence on the amplification

rate $\omega_i(k_r)$, even for $F > 4$, rare values to be naturally observed by the literature.

From the point of view of the spatial stability analysis, regarding the spatial growth rate ($k_i(\omega_r)$), there is a singularity point of the function, which was defined as F_s . According to the discussions presented, this parameter contributes to the change in behavior of the instability growth rate.

In general, it is concluded that the fluid flow index (n) affects the growth or decrease of the amplification rate, either in the time domain or in the spatial domain. For the temporal analysis, it can be seen that amplification rates increase for $n < 1$ and decrease for $n > 1$. For the spatial analysis, the behavior is the opposite: the rates decrease for $n < 1$ and increase for $n > 1$.

Finally, based on the results obtained so far, we intend to carry out further mathematical investigations regarding the evolution of instabilities for the Herschel-Bulkley rheological model, to point out the characteristics conditioned by the yield stress in the propagation of hydrodynamic instabilities.

5. ACKNOWLEDGEMENTS

Valdirene da Rosa Rocho thanks the Sombrio Advanced Campus of the Catarinense Federal Institute for granting a full time leave for doctoral studies, via notice No. 21/2019.

6. REFERENCES

- Balmforth, N. and Liu, J., 2004. "Roll waves in mud". *Journal of Fluid Mechanics*, Vol. 519.
- Briggs, R.J., 1964. *Electrons-Stream Interaction with Plasmas*. MIT Press, Massachusetts.
- Charru, F., 2011. *Hydrodynamic Instabilities*. Cambridge Texts in applied Mathematics, Cambridge.
- Di Cristo, C. and Vacca, A., 2005. "On the convective nature of roll waves instability". *Journal of Applied Mathematics*, Vol. 2005, pp. 259–271.
- Di Cristo, C., Iervolino, M. and Vacca, A., 2017. "A strategy for passive control of natural roll-waves in power-law fluids through inlet boundary conditions". *Journal of Applied Fluid Mechanics*, Vol. 10, pp. 667–680.
- Dressler, R.F., 1949. "Mathematical solution of the roll-waves in inclined open channels". *Communications on Pure and Applied Mathematics*, Vol. 2, pp. 149–194.
- Huerre, P. and Monkewitz, P.A., 1990. "Local and global instabilities in spatially developing flows". *Annual Review of Fluid Mechanics*, Vol. 22, No. 1, pp. 473–537.
- Irgens, F., 2014. *Rheology and Non-Newtonian Fluids*. Springer International Publishing Switzerland, New York.
- Ishihara, T., Iwagaki, Y. and Iwasa, Y., 1954. "Theory of the roll-wave trains in laminar water flow on a steep slope surface". *Transactions of the Japanese Society of Civil Engineer*, Vol. 1954, No. 19, pp. 46–57.
- Jeffreys, H., 1925. "LXXXIV. the flow of water in an inclined channel of rectangular section". *The London, Edinburgh, and Dublin Philosophical Magazine and Journal of Science*, Vol. 49, No. 293, pp. 793–807.
- Julien, P.Y. and Hartley, D.M., 1986. "Formation of roll waves in laminar sheet flow". *Journal of Hydraulic Research*, Vol. 24, No. 1, pp. 5–17.
- Liu, K.; Mei, C., 1994. "Roll waves on a layer of a muddy fluid flowing down a gentle slope – a bingham model." *Physics of Fluids*, Vol. 6, No. 8, pp. 2577–2589.
- Longo, S., 2011. "Roll waves on a shallow layer of a dilatant fluid". *European Journal of Mechanics B/Fluids*, Vol. 30, pp. 57–67.
- Maciel, G.F., Ferreira, F.O. and Fiorot, G.H., 2013. "Control of instabilities in non-newtonian free surface fluid flows". *Journal of the Brazilian Society of Mechanical Sciences and Engineering*.
- Needham, D.J. and Merkin, H., 1984. "On roll waves down an open inclined channel". *Journal Mathematical Physical & Engineering Sciences*, Vol. 394, pp. 259–278.
- Ng, C.O. and Mei, C.C., 1994. "Roll waves on a shallow layer of mud modelled as a power-law fluid". *Journal of Fluid Mechanics*, Vol. 263, pp. 151–184.
- Pascal, J., 2006. "Instability of power-law fluid flow down a porous incline". *Journal of Non-Newtonian Fluid Mechanics*, Vol. 133, No. 2, pp. 109–120. ISSN 0377-0257.
- Tamada, K. and Tougou, H., 1979. "Stability of roll-waves on thin laminar flow down an inclined plane wall". *Journal of the Physical Society of Japan*, Vol. 47, No. 6, pp. 1992–1998.
- Zanuttigh, B. and Lamberti, A., 2007. "Instability and surge development in debris flows". *Reviews of Geophysics*, Vol. 45, No. 3, pp. 1–45. ISSN 8755-1209.
- Zanuttigh, B. and Lamberti, A., 2010. "Roll waves simulation using shallow water equations and weighted average flux method". *Journal of Hydraulic Research*, Vol. September 2002, pp. 610–622.

7. RESPONSIBILITY NOTICE

The authors are solely responsible for the printed material included in this paper.